Tong and Liu *Chin. J. Mech. Eng.* (2018) 31:62
https://doi.org/10.1186/s10033-018-0261-2

Chinese Journal of Mechanical Engineering

ORIGINAL ARTICLE

Open Access

Nanoscale Reciprocating Sliding Contacts of Textured Surfaces: Influence of Structure Parameters and Indentation Depth

Rui-Ting Tong* and Geng Liu

Abstract

Textured surfaces are widely used in engineering components as they can improve tribological properties of sliding contacts, while the detailed behaviors of nanoscale reciprocating sliding contacts of textured surfaces are still lack of study. By using multiscale method, two dimensional nanoscale reciprocating sliding contacts of textured surfaces are investigated. The influence of indentation depth, texture shape, texture spacing, and tip radius on the average friction forces and the running-in stages is studied. The results show that the lowest indentation depth can make all the four textured surfaces reach steady state. Surfaces with right-angled trapezoid textures on the right side are better for reducing the running-in stage, and surfaces with right-angled trapezoid textures on the left side are better to reduce wear. Compared with other textured surfaces, the total average friction forces can be reduced by 82.94%–91.49% for the case of the contact between the tip with radius $R=60r_0$ and the isosceles trapezoid textured surface. Besides, the total average friction forces increase with the tip radii due to that bigger tip will induce higher contact areas. This research proposes a detailed study on nanoscale reciprocating sliding contacts of textured surfaces, to contribute to design textured surfaces, reduce friction and wear.

Keywords: Nanoscale, Reciprocating sliding contacts, Textured surface, Structure parameters, Indentation depth

1 Introduction

Textured surfaces were widely used in many engineering areas, such as automotive components, bearings, mechanical seals, cutting tools, magnetic disks, and artificial joints, etc., due to their potential to improve tribological characteristics. Besides the studies on the applications above, many works have been carried out to investigate the detailed behaviors of textured surfaces in reciprocating sliding contacts.

The influence of structure parameters of textured surfaces on the frictional properties of reciprocating sliding contacts were widely investigated. Menezes et al. [1, 2] slid Al-4Mg alloys pins against textured steel plates, and they pointed out that coefficient of friction (COF) mainly depended on the change in texture of surfaces rather than roughness. Diamond-like carbon (DLC) coating was coated on the textured surfaces of silicon wafers, and 5 and 20 μm grooved textures in the reciprocating sliding contacts showed excellent performance [3]. According to the results of tests, Kovalchenko et al. [4] found that higher dimple density induced higher COFs compared with the disc with standard dimple density. Ramesh et al. [5] investigated frictional characteristics of textured surfaces on stainless steel surfaces. Friction forces decreased as the increase of texture density. Scaraggi et al. [6] studied the frictional properties of lubricated laser micro-textured surfaces. They found that the depth and diameter of the micro-holes greatly influenced friction reduction at the interface. In Ref. [7], the influence of chevron-shaped textures on frictional behaviors of carbon manganese steel plate was investigated, and the friction decreased as the increase of the chevron texture density. Fan et al. [8] fabricated micro-dimples with different area densities on the Si-DLC films of Al2O3/Ni laminated composites, and the COF could be reduced by nearly one order of magnitude. In the work of He et al. [9], an appropriate

*Correspondence: tongruiting@nwpu.edu.cn; nputongruiting@163.com
Shaanxi Engineering Laboratory for Transmissions and Controls, Northwestern Polytechnical University, Xi'an 710072, China

number of dimples on the DLC surface could reduce friction and wear rate. Line-, cross-, and dot-like patterned surfaces were employed in the research of Bieda et al. [10], and patterned surfaces could reduce COFs by 25 to 65% compared with unpatterned surfaces. In Ref. [11], microtextures were created on the surface of TC11 alloy, and a relative small diameter and dense micro-dimpled structure were likely to improve the wear resistance of the TC11 alloy under 500 °C environment temperature. Wang et al. [12] investigated the effects of surface textures on point-contact lubrication. The textures with big side length perpendicular to the sliding direction were recommended to reduce friction.

Sliding parameters, applied load, and some other factors will also influence the reciprocating sliding processes. The work of Zum Gahr et al. [13], showed that the beneficial effects of surface texture depended on loading, geometry and lubrication conditions as well as the materials and surface textures involved. In Ref. [14], the frictional behaviors of ground, polished, and LST discs with different texture density and depth were studied. For low sliding speed, significant differences of frictional performance were observed, while the difference was insignificant for high sliding speed. Zum Gahr et al. [15] found that increasing normal load, area coverage fraction, depth and width of crossed microchannels as well as decreasing sliding velocity would increase friction. Frictional behaviors of parallel grooves, random grooves and polished surfaces were investigated in Ref. [16]. Polished surface got higher average COF than the other two textures, and the COFs for all the three textures were higher under low load than under high load. Furthermore, the direction of surface texture had significant effects on film thickness that would influence friction behaviors.

Most of the textures in the studies above are microscale, while the behaviors of nanoscale textures will be important in nanoelectromechanical systems as they can vary area-to-volume ratio and influence adhesive effects. Zhang et al. [17] performed experiments on nanotextured silicon surface by using atomic force microscope (AFM), and the results showed a strong dependence of COF on tip radius and sliding direction. Kim et al. [18] investigated nanoscale frictional behaviors of corrugated nano-structured surfaces by molecular dynamics (MD) simulations. COF of the nano-structured surface was lower than that of a smooth surface, and the influence of applied load on the COF depended on the size of the corrugation. MD simulation was also used to study the nanoscale high speed grinding process of single crystal copper with textured surface in Ref. [19]. The results showed that texture shape influenced the volume of material pileups and chips greatly. Tong et al. [20] studied the sliding contacts between rigid cylindrical tips and textured surfaces by multiscale method, and the surfaces with trapezoid textures could reduce friction forces more effectively. It should be noted that most of the studies on nanoscale textures were single-pass, while the work of Mitchell et al. [21] pointed out that the single-pass COF measurements were not good predictions of the steady state COF values measured in reciprocating friction. The author investigated nanoscale reciprocating sliding contacts of textured surfaces, and observed the steady state sliding process, while the effects of structure parameters of textures and other parameters on reciprocating frictional behaviors were still unclear. Therefore, it is interesting to know the reciprocating frictional properties of nanoscale textured surfaces during reciprocating sliding contacts under different parameters.

In this paper, a multiscale method [22], which could save much CPU time, was used to investigate nanoscale reciprocating sliding contacts between rigid cylindrical tips and textured surfaces. Four textured surfaces with different shapes were designed, and three tips with different radii were used to slide on textured surfaces. As the sliding numbers increased, the variation of average friction forces were given, and the effects of texture shape, texture spacing, tip radius and indentation depth on the average friction forces, the running-in stages and the wear properties were discussed.

2 Model Descriptions

A multiscale model was presented in Figure 1 to investigate nanoscale reciprocating sliding contacts between rigid cylindrical tips and textured surfaces. The model included a rigid cylindrical tip whose radius was $R=30r_0$ (r_0 was the Lennard-Jones parameter, $r_0=0.2277$ nm [23]

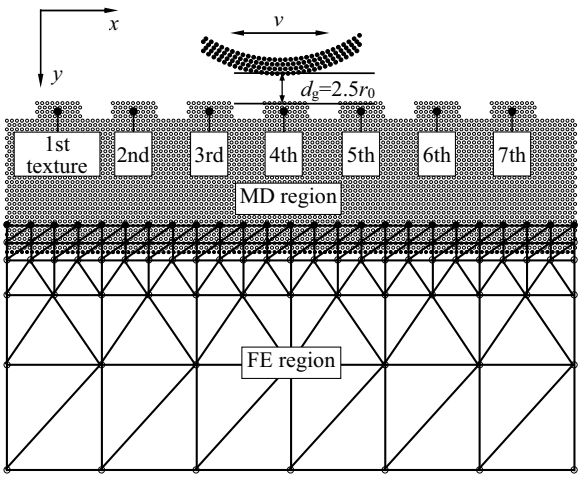

Figure 1 Nanoscale reciprocating sliding contact model between a rigid cylindrical tip and a textured surface

here), and an elastic substrate whose scale was $112.5d_x \times 80.0d_y$ besides the textures, where $d_x = \sqrt[6]{2}r_0$, was the distance between two adjacent atoms in x direction, and $d_y = \sqrt{3}/2 \times d_x$, was the distance between two adjacent layers in y direction. The rigid cylindrical tip consisted of 4 layers with 120 atoms, and the substrate was divided to two parts: MD region and finite element (FE) region. For the MD region, there were 3503 atoms (31 layers and 113 atoms per layer) and 7 textures on the surface. For the FE region, there were 102 nodes and 162 triangular finite elements totally. Initial gap between the tip and substrate was $d_g = 2.5r_0$. Textures on the substrate were named as the "1st texture", "2nd texture", ..., and "7th texture".

To investigate the influence of textured surfaces, four textured surfaces with different shapes were used in this paper. The parameters of the textured surfaces were designed as width $a = 8d_x$, spacing $b = 7d_x$, and height $h = 4d_y$, as shown in Figure 2. The four textured surfaces were named as surface I, II, III and IV, respectively. For surface I, the number of atoms in each layer of a single texture was, $m_A = 9$. For surface II, the number of atoms from bottom layer to top layer of each single texture was changed from, $m_A = 9$, to 8, 7 and 6, etc. The numbers were 9, 9, 8 and 8 for the textures of surfaces III and IV. The number of textures for these four textured surfaces was $n_A = 7$.

A multiscale method [22] which coupled MD simulation and FE method was used to simulate this reciprocating sliding contact problem. For MD simulations, Lennard-Jones (L-J) potential was used to describe interactions among all the atoms:

$$U(r_{ij}) = 4\varepsilon \left[\left(\frac{r_0}{r_{ij}} \right)^{12} - \left(\frac{r_0}{r_{ij}} \right)^{6} \right], \quad r_{ij} \le r_c, \tag{1}$$

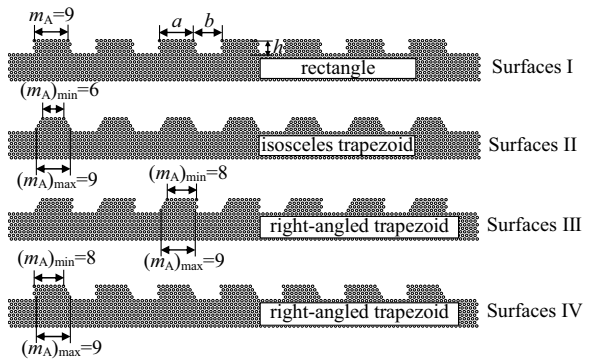

Figure 2 Topographies of textured surfaces

where $r_{ij} = \|\boldsymbol{r}_i - \boldsymbol{r}_j\|$, denoted the distance between atoms i and j, ε and r_0 were the L-J parameters. For FCC Cu, $\varepsilon = 6.648 \times 10^{-20}$ J, $r_0 = 0.2277$ nm [23]. The cut-off radius, $r_c = 2.2r_0$ according to Ref. [24] here. Atoms on the bottom layer of the MD region were fixed temporarily before the simulation. For two atoms i and j, the force that atom j exerted on atom i could be written as follows:

$$\begin{aligned} \boldsymbol{F}(r_{ij}) &= -\nabla U(r_{ij}) \\ &= \left(\frac{48\varepsilon}{r_0^2} \right) \left[\left(\frac{r_0}{r_{ij}} \right)^{14} - \frac{1}{2} \left(\frac{r_0}{r_{ij}} \right)^{8} \right] \boldsymbol{r}_{ij}, \quad r_{ij} \le r_c. \end{aligned} \tag{2}$$

Velocity-Verlet algorithm [25] was used to calculate coordinates, velocities, and accelerations of all the atoms:

$$\begin{cases} \boldsymbol{r}(t + \Delta t) = \boldsymbol{r}(t) + \boldsymbol{v}(t)\Delta t + \dfrac{1}{2}\boldsymbol{a}(t)\Delta t^2, \\ \boldsymbol{v}(t + \Delta t/2) = \boldsymbol{v}(t) + \dfrac{1}{2}\boldsymbol{a}(t)\Delta t, \\ \boldsymbol{a}(t + \Delta t) = -\dfrac{1}{m}\nabla U(\boldsymbol{r}(t + \Delta t)), \\ \boldsymbol{v}(t + \Delta t) = \boldsymbol{v}(t + \Delta t/2) + \dfrac{1}{2}\boldsymbol{a}(t + \Delta t)\Delta t, \end{cases} \tag{3}$$

where Δt was time step, $\boldsymbol{r}$ was coordinate vector, $\boldsymbol{v}$ was velocity vector, $\boldsymbol{a}$ was acceleration vector, and m was mass of an atom.

When the MD simulations were carried out for every $50\Delta t$, displacements of the topmost FE nodes were calculated through displacements of atoms around the FE nodes. The displacements of these FE nodes were then used as initial conditions for FE calculations. Quasi-static elastic constitutive relationship and Newton–Raphson iteration were employed due to that displacements of the FE region were very small compared with those in the MD region. When FE calculation was finished, the displacements of atoms on the bottom layer could be obtained according to their positions in the corresponding elements, and the positions of the atoms were updated by using their displacements. So, one could obtain a new MD region and perform MD simulations again. More detailed working processes about multiscale method were given in Ref. [22].

3 Results and Discussion

During the simulation of indentation and sliding processes, coordinates, velocities, and accelerations of all the atoms were calculated by velocity-Verlet algorithm, and a fixed time step, $\Delta t = 0.95$ fs was used. Initially, velocities of all the atoms except fixed boundary ones were set with random Gaussian distribution under an equivalent temperature $T = 300$ K. Before loading, the MD system

was relaxed to reach its minimum energy configuration. Then, the tip moved to the substrate in y direction with a displacement increment $\Delta s = 0.05r_0$ and the indentation speed was $v = 2.0$ m/s. When the indentation process finished, the tip slid along x direction, and the sliding speed was also $v = 2.0$ m/s. In MD simulations, high sliding speed might result in biased results [26], so the sliding speed was chosen as $v = 2.0$ m/s here. The tip moved to right (forward sliding, odd sliding numbers) for $320\Delta s$, and then it moved to left (backward sliding, even sliding numbers) for $320\Delta s$. The forward and backward sliding processes were carried out for 10 times, respectively.

3.1 Effects of Indentation Depth and Texture Shape

To investigate the effects of indentation depth, three cases including $d = 3.0r_0$, $d = 2.5r_0$ and $d = 2.0r_0$ are chosen. The indentation depth is defined as the value that the final coordinate minus the original coordinate of the tip in y direction. When the indentation depth is $d = 3.0r_0$, average friction forces of the four textured surfaces are shown in Figure 3. For surface I, the 4th and 5th textures are scratched to form a big texture when the 2nd sliding finishes, and the tip is covered by one layer atoms from textures. After the 6th sliding, the cover layer fractures, and only the right part of the cover layer contacts with the big texture, so the friction forces of the 7th to 16th slidings are lower than the cases of the 3rd to 6th slidings. In the periods of the 7th to 16th slidings, a short steady state is occurred, as shown in Figure 4(a), and attractive forces from the 6th texture induce the difference of the average friction forces between odd and even sliding numbers. When the 17th sliding begins, several atoms of the right part of the cover layer are moved to the left part, and the left part contacts with the big texture then. The regular sliding process is broken, and the average friction forces fluctuate unregularly then.

When the tip slides on surface II, atoms of the textures are not enough to fill the spacing, and the big texture is not formed until the 16th sliding. Also, because atoms of the textures are fewer than the other cases, the big texture only contains one layer, and the sliding process still not come to steady state, so the average friction forces fluctuate during all this period, as shown in Figure 3(b). Additionally, the big texture gets one layer, as shown in Figure 4(b), which makes larger gap between the tip and the big texture compared with the other cases, and there are fewer atoms between the tip and the big texture to induce less interactions. Therefore, the average friction forces at the final stage are lower.

For surface III, the sliding contact comes to steady state since the 6th sliding. 3 atoms adhere to the left part of the tip, and 7 atoms adhere to the right part of the tip, which is shown in Figure 4(c). Attractive forces from the 6th texture will make contributions to the tip to slide to the right for odd sliding numbers, while the forces will be resistance for the cases of even sliding numbers. Therefore, the attractive forces induce the difference between

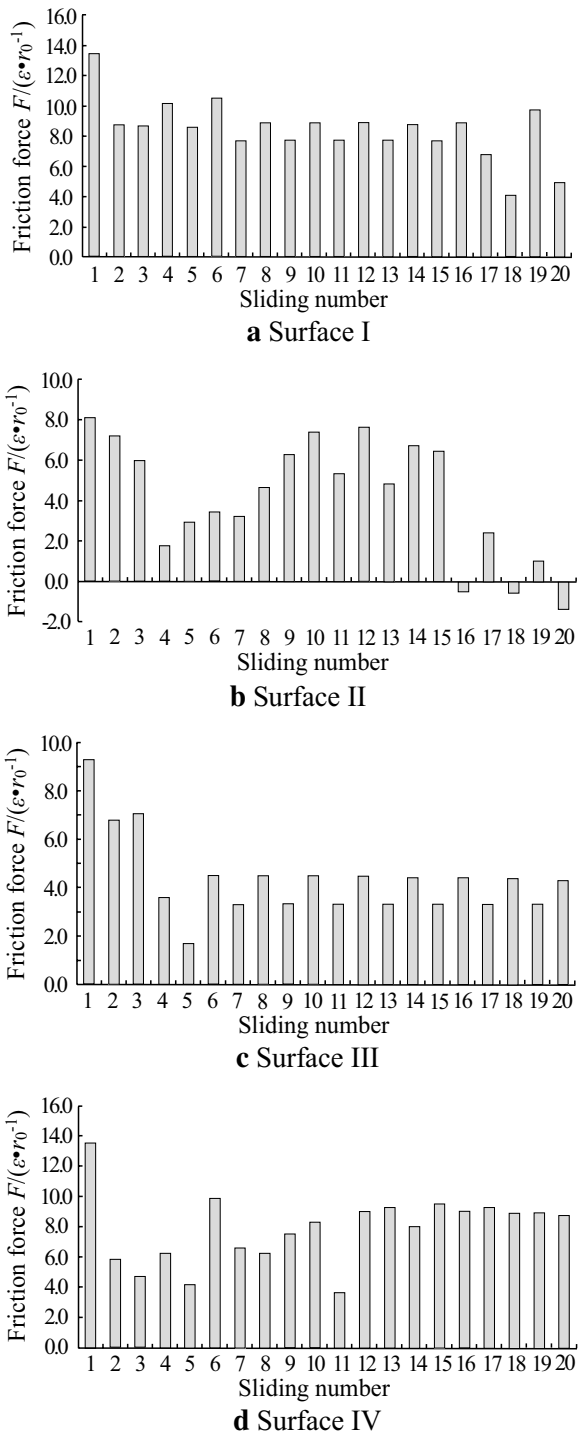

Figure 3 Nanoscale reciprocating sliding contacts of textured surfaces (7 textures, $R = 30r_0$, $d = 3.0r_0$)

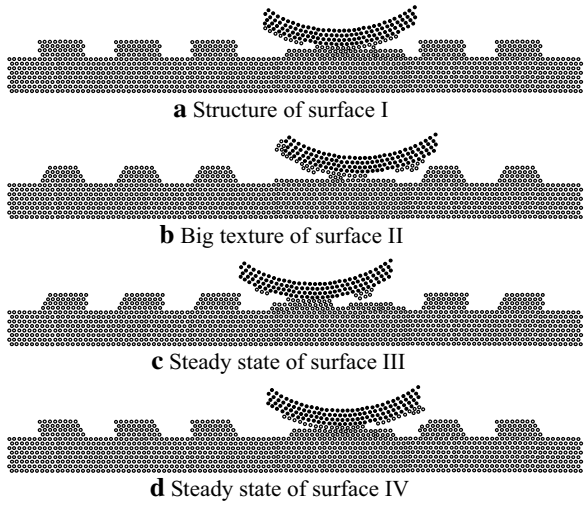

Figure 4 Structures during reciprocating sliding processes of textured surfaces (7 textures, $R=30r_0$, $d=3.0r_0$)

the average friction forces in steady state for different sliding numbers.

The tip scratches the 4th and 5th textures to fill the spacing between the two textures for surface IV, and adhered atoms on the tip form a layer which covers the contact surface of the tip gradually. A big texture consisted of two layers is formed, as shown in Figure 4(d), and the tip takes the cover layer to slide on the big texture to show the steady average friction forces since the 15th sliding in Figure 3(d).

Comparing these 4 textured surfaces, surface I and surface II do not come to steady state, while surface III and surface IV reach steady state. The running-in stage is 5 slidings for surface III, which is shorter than surface IV. As a result, surface III contributes to reducing the running-in stage during the sliding processes. Besides, the average friction forces of surface III is also lower than other cases except for the final stage of surface II. Moreover, for surface II, more atoms are taken away by the tip, and the wear property is the worst among the four textured surfaces. Therefore, we can conclude that surface III should be better to reduce friction and the running-in stage under the initial conditions in this section.

When the indentation depth is $d=2.5r_0$, average friction forces are shown in Figure 5. From the theory of Ref. [27], one can find that scratches from the tip are lower than the case of $d=3.0r_0$. So, for surface I, the big texture is not formed so quickly as the case of $d=3.0r_0$. Although a big texture is formed when the 3rd sliding is completed, the sliding process does not reach steady state because the big texture and the cover layer on the tip are changed all the time. In the following slidings, atoms adhered on

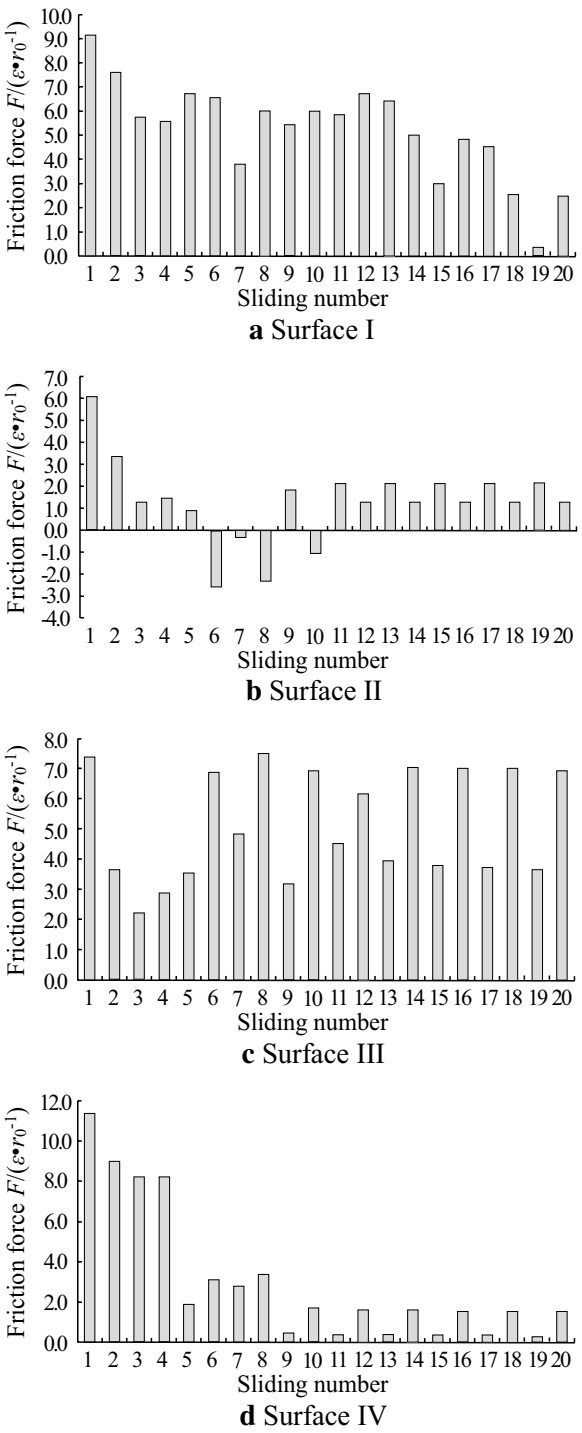

Figure 5 Nanoscale reciprocating sliding contacts of textured surfaces (7 textures, $R=30r_0$, $d=2.5r_0$)

the tip accumulate on the left side of the 6th texture, as shown in Figure 6(a), and atoms of the cover layer on the tip are fewer than the former sliding processes. During

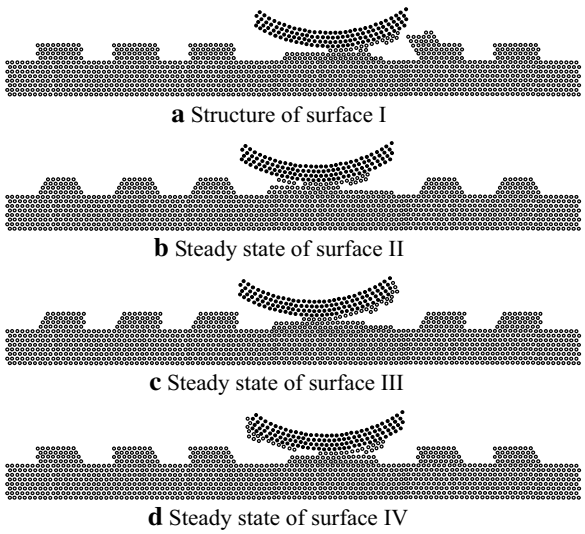

Figure 6 Structures during reciprocating sliding processes of textured surfaces (7 textures, $R=30r_0$, $d=2.5r_0$)

the 19th sliding, attractive forces from the 6th texture act on the tip in the same direction as the sliding, so the average friction force is the lowest. Then the attractive forces act in the opposite direction to the 20th sliding, and the average friction force is higher than the 19th sliding.

For surface II, the tip takes several atoms to slide together on the 4th and 5th textures as the 1st sliding begins. It is difficult to form a big stable texture due to the small number of atoms in a single texture. A big texture is formed after the 10th sliding, and the big texture consists of two parts. As shown in Figure 6(b), the left part includes 2 layers atoms, and the right part gets 1 layer atoms, so, attractive forces produced by the left part are higher than the right part. For odd sliding, attractive forces from the left part act on the tip in the opposite direction of the sliding, while the attractive forces get the same direction with the sliding direction for even sliding, so the average friction forces for odd slidings are higher than the cases of even slidings. From the 11th sliding, the tip takes atoms to slide on this big texture, and the average friction forces for odd or even slidings are stable until final stage.

When the tip slides on surface III, the topmost two layers of the 4th and 5th textures are scratched by the tip, and some atoms are filled into the spacing between the two textures. As the sliding going on, a big stable texture is formed since the 13th sliding, and only the right part of the tip is covered by adhered atoms, as shown in Figure 6(c). The interactions between the tip with its cover layer and the big texture make the difference of average friction forces for odd or even slidings. There are attractive forces acting on the tip and its cover layer from the big texture. The direction of the composition of attractive forces is same as the odd sliding because the right part of the current tip gets more atoms than the left part considering the cover layer. Therefore, the average friction forces of the odd slidings are lower than the cases of even slidings.

For surface IV, the tip takes the whole 4th texture to connect to the 5th texture in the 1st sliding, and a big texture is formed soon. Although the big texture gets stable structure, the cover layer of the tip is not stable until the 9th sliding. As shown in Figure 6(d), the cover layer is divided to left part and right part, and the left part does not contact with the big texture. As a result, the interactions between the tip with the cover layer and the big texture are low, which induces lower average friction forces than the other three cases.

Under the indentation depth $d=2.5r_0$, textured surfaces II, III and IV all come to steady state, and the running-in stages are 10, 12, and 8 sliding processes, respectively. From the view of reducing the running-in stage, surface IV could be a better choice. Furthermore, in the steady state, surface IV shows the lowest average friction forces among these four surfaces, which will improve frictional characteristics during reciprocating sliding contacts. Therefore, under these initial conditions, surface IV should be the best to improve tribological characteristics. Considering the wear properties, one can find that 35 atoms of surface I are taken away by the tip, which is most among the four textured surfaces. As a result, surface I is not suitable to reduce friction and wear.

When the indentation depth is $d=2.0r_0$, average friction forces are shown in Figure 7. Due to lower indentation depth, ploughing component of friction force becomes lower than the cases of $d=2.5r_0$ or $d=3.0r_0$, and adhesion component plays more important role. Therefore, one can find that the highest friction forces are all lower than the corresponding cases of $d=2.5r_0$ or $d=3.0r_0$.

For surface I, the tip takes part of the 4th and 5th textures to slide together, and a big texture is not formed until the end of the 9th sliding. From the 10th sliding, the steady state occurs, and average friction forces for odd or even slidings are also stable. As shown in Figure 8(a), the left part of the cover layer includes more atoms than the right part, so interactions between the left part and the big texture are greater than the right part. When the tip slides to right (odd sliding), the direction of composition forces is opposite to the sliding direction, so the average friction forces are positive. On the contrary, the two directions are the same when the tip slides to left (even sliding), and the average friction forces show negative values.

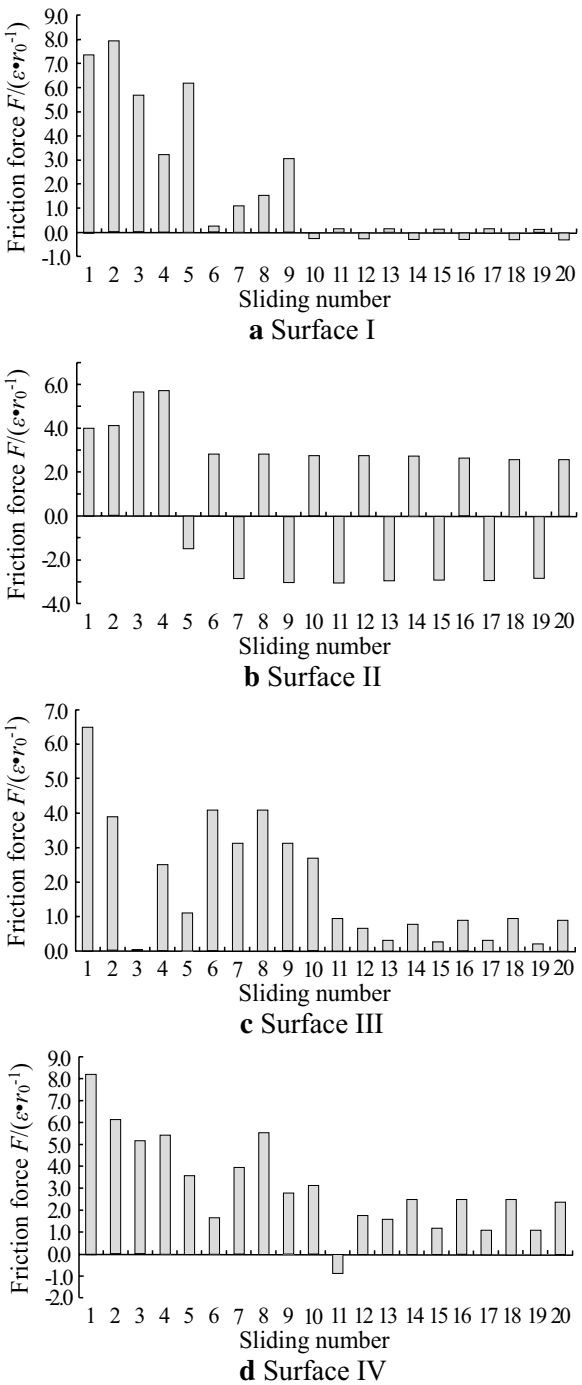

Figure 7 Nanoscale reciprocating sliding contacts of textured surfaces (7 textures, $R = 30r_0$, $d = 2.0r_0$)

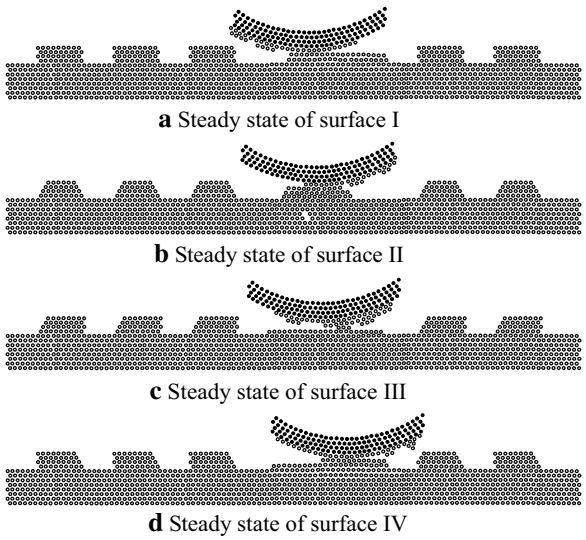

Figure 8 Structures during reciprocating sliding processes of textured surfaces (7 textures, $R = 30r_0$, $d = 2.0r_0$)

For the case of surface II, the tip scratches the topmost layers of the 4th and 5th textures during the 1st sliding, and the 5th texture is taken by the tip to connect to the 4th texture in the 2nd sliding. After 5 slidings, a big texture is formed, and the cover layer mainly adheres to the right part of the tip, which is shown in Figure 8(b). As a result, the direction of the composition of the attractive forces is opposite to the direction of even slidings (left), so the average friction forces get positive values. The attractive forces acting on the tip are in the same direction of odd slidings to make negative average friction forces.

The tip takes the topmost layer of the 4th texture to slide together and scratches the 5th texture in the 1st sliding for the case of surface III. As the sliding going on, a big texture which includes 1 layer atoms is formed after 6 slidings, but the structure of cover layer on the tip is still not stable until the end of the 11th sliding. As shown in Figure 8(c), the cover layer mainly includes 2 layers except some region of the left part. Besides, in the contact region between the tip and the substrate, the cover layer contains 3 layers, and there are more atoms adhered to the tip on the right part than the left part. When the tip slides to right (odd slidings), attractive forces from the 6th texture act on the same direction with the sliding, so the average friction forces are low, while the average friction forces are high for the cases of even slidings.

For surface IV, the tip does not take the 4th or the 5th textures to slide, instead it takes some atoms of these two textures to slide together. When the 9th sliding is finished, a big texture is formed, but the cover layer is still not stable. As the sliding going on, a stable big texture which contains 1 layer on the left part and 2 layers on the right part is formed after the 12th sliding. As shown in Figure 8(d), the tip is covered by one layer with some more atoms on the right part, so attractive forces

between the substrate and the left part are lower than the right part. From the 13th sliding, when the tip slides to right (odd sliding), average friction forces are low because an attractive force acts on the tip in the same direction as the sliding. On the contrary, the average friction forces are high when the tip slides to left.

For these four textured surfaces, more atoms are worn when the tip slides on surface III. Comparing Figures 3, 5 and 7, one can find that there are 2, 3, and 4 surfaces reaching steady state corresponding to the indentation depth $d=3.0r_0$, $d=2.5r_0$, and $d=2.0r_0$, and the lowest indentation depth makes all the sliding processes come to steady state. Besides, both surfaces III and IV reach steady state for all the indentation depth in this work, which indicates that surfaces III and IV could be better choices to reducing running-in stage. From the view of wear property, surfaces I, II and III show the worst behaviors under different indentation depth respectively, which indicates that surface IV is the best to reduce wear.

3.2 Effects of Texture Spacing

The spacing between two neighbor textures will trap wear atoms and influence the formation of big texture. In this section, we change the spacing to $b=4d_x$, then there are 9 textures on the substrate, and the sliding processes mainly relate to the 5th, 6th and 7th textures. The indentation depth is $d=2.5r_0$, and the other parameters of the model are the same as Section 3.1. The average friction forces for different surfaces are shown in Figure 9.

For surface I, the 5th, 6th and 7th textures connect together to form a big texture during the 1st sliding. The spacing between two textures is so small that there are too many atoms between the tip and the substrate, which makes the structure of the big texture and cover layer change all the time. Atoms accumulate in the region of the 7th texture, and the tip contacts with accumulated atoms when it slides to right. As shown in Figure 10(a), when the 13th sliding is completed, a peak, which is higher than original textures, is formed around the region of the 7th texture. During the 14th sliding, the tip must break the connection from the peak, so the average friction force is high. Similarly, the average friction forces of even slidings are higher than the odd slidings.

The tip takes some atoms of textures to slide together during the former 3 slidings for surface II, and a big texture which consists of 2 layers is formed at the end of the 4th sliding. Atoms scratched by the tip begin to accumulate on the top of the 7th texture. Similar to the case of surface I, the tip contacts with the current 7th texture. From the 8th sliding, when the tip slides to left (even sliding), it must break the connection between the tip and the 7th texture, so the average friction forces of even slidings are higher than the odd slidings. From the 13th sliding, a big texture and the cover layer of the tip come to stable structures which are shown in Figure 10(b), and the average friction forces also keep stable corresponding to the odd or even slidings.

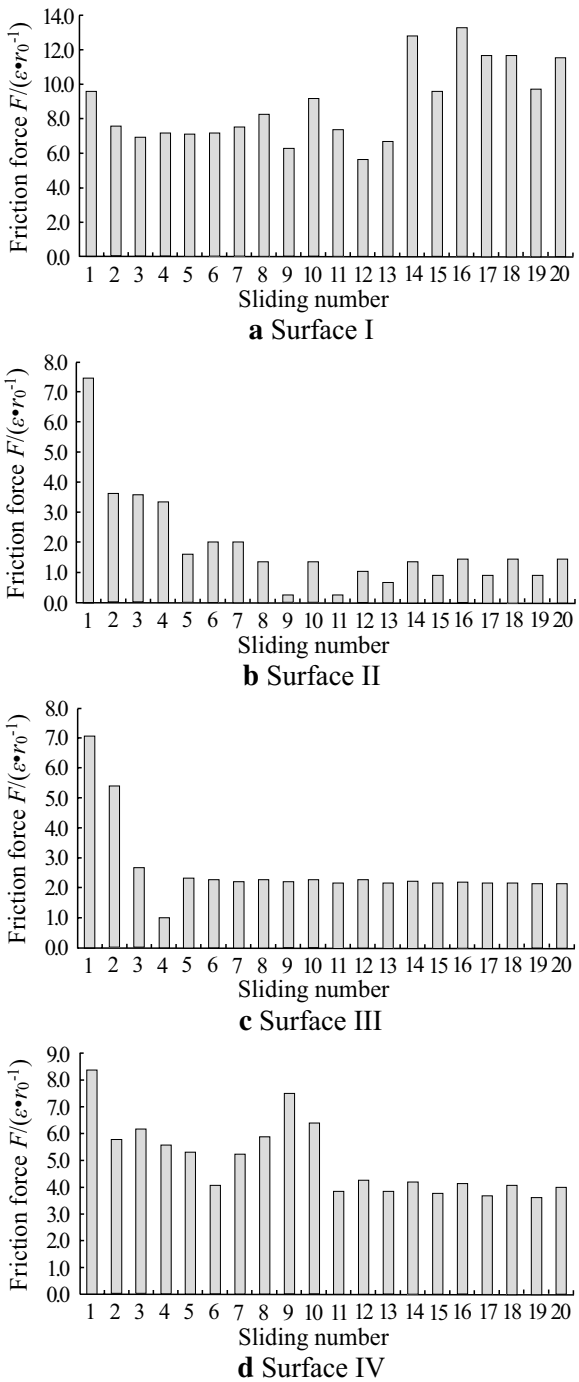

Figure 9 Nanoscale reciprocating sliding contacts of textured surfaces (9 textures, $R=30r_0$, $d=2.5r_0$)

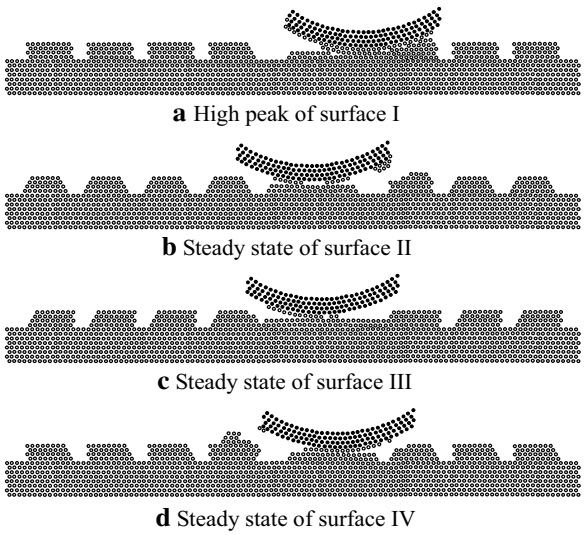

Figure 10 Structures during reciprocating sliding processes of textured surfaces (9 textures, $R=30r_0$, $d=2.5r_0$)

For surface III, atoms of the 5th and 6th textures are scratched to fill the spacings between the 5th, 6th and 7th textures in the 1st sliding. A big texture is formed when the 3rd sliding is finished, and the structures of the big texture and cover layer are stable after the 4th sliding. As shown in Figure 10(c), the big texture includes 2 layers, and the tip slides on this big texture all the time during the stable sliding processes. Therefore, average friction forces keep stable from the 5th sliding.

The tip takes the whole 5th texture to join the 6th texture during the 1st sliding for surface IV, and these two textures form a big texture. As the sliding going on, the big texture includes 2 layers and comes to steady state, and the cover layer also gets a stable structure. Atoms taken by the tip accumulate on the top of the 4th texture gradually, which induces that the tip contacts with the 4th texture and the accumulated atoms. From the 11th sliding, the sliding processes come to steady state, and average friction forces for even slidings are a little higher than the cases of odd slidings. This phenomenon is caused by the contacts between the tip and the 4th texture including its accumulated atoms, as shown in Figure 10(d). For the even slidings, the tip scratches the 4th texture and its accumulated atoms, which induces high friction forces due to high ploughing components.

Comparing Figure 5 and Figure 9, surfaces II, III and IV all reach steady state for these two different texture spacings, and there are no obvious trends for the influence of texture spacing. According to the sliding processes, one can find that, atoms scratched by the tip can be filled into the spacings, and big textures can be formed during the slidings. Although surfaces with 9 textures get more atoms, some of the atoms accumulate outside or at the edge of contact region. Therefore, the effects of texture spacing on friction forces show no regular trends. From Figure 6 and Figure 10, one can find that the worn atoms of surface I with 9 textures are obviously more than the case of 7 textures, and the wear behavior of surface I is the worst. Similar to Section 3.1, surface I with 9 textures is not suitable to reduce friction and wear.

3.3 Effects of Tip Radius

For a given texture, tip radius will influence interactions between the tip and textures. To study the effects of tip radius, $R=60r_0$ and $R=120r_0$ are chosen in this section, and the corresponding atoms of these two tips are 240 and 480. The indentation depth is $d=2.5r_0$, and the other parameters are same as Section 3.1.

Figure 11 shows the average friction forces for the tip of $R=60r_0$ sliding on the four textured surfaces. For surface I, the tip takes the whole 4th texture to connect to the 5th texture in the 1st sliding, and a big texture which includes 4 layers is formed, as shown in Figure 12(a). From the 2nd sliding to the final stage, the tip takes the whole big texture to slide together for a distance besides sliding on the big texture. For the 2nd to the 6th slidings, the tip takes the big texture to slide for $9.5d_x$, while the distance is $8.5d_x$ for the cases of the 7th sliding to the final stage. When the tip takes the big texture to slide together on the substrate, the width of the big texture can be taken as contact area, and the contact area is higher than the case that the tip slides on the big texture. Therefore, the average friction forces during the 2nd to the 6th slidings are higher than the cases of the following slidings.

For surface II, textures include fewer atoms than surface I, so the spacing is difficult to be filled. Besides, as the tip radius is $R=60r_0$, many atoms adhere to the tip, and the substrate only gets a few atoms, which limits the formation of the big texture. Furthermore, the cover layer dose not form a stable structure through all the sliding processes, so the average friction forces fluctuate unregularly during all the 20 slidings.

For surface III, the tip takes the 4th texture to slide towards the 5th texture, and these two textures join together to form a big texture in the 1st sliding. During the 3rd and 4th slidings, the cover layer on the tip gets its stable structure shown in Figure 12(b), and the sliding comes to steady state from the 5th sliding. Then, for the odd slidings, the tip breaks the big texture and takes part of the big texture to slide together, which is shown in Figure 12(c). The tip must overcome forces to break the big texture, which induces high average friction forces for odd slidings. When the tip slides to left (even sliding), it takes the broken part of the big texture to slide back to

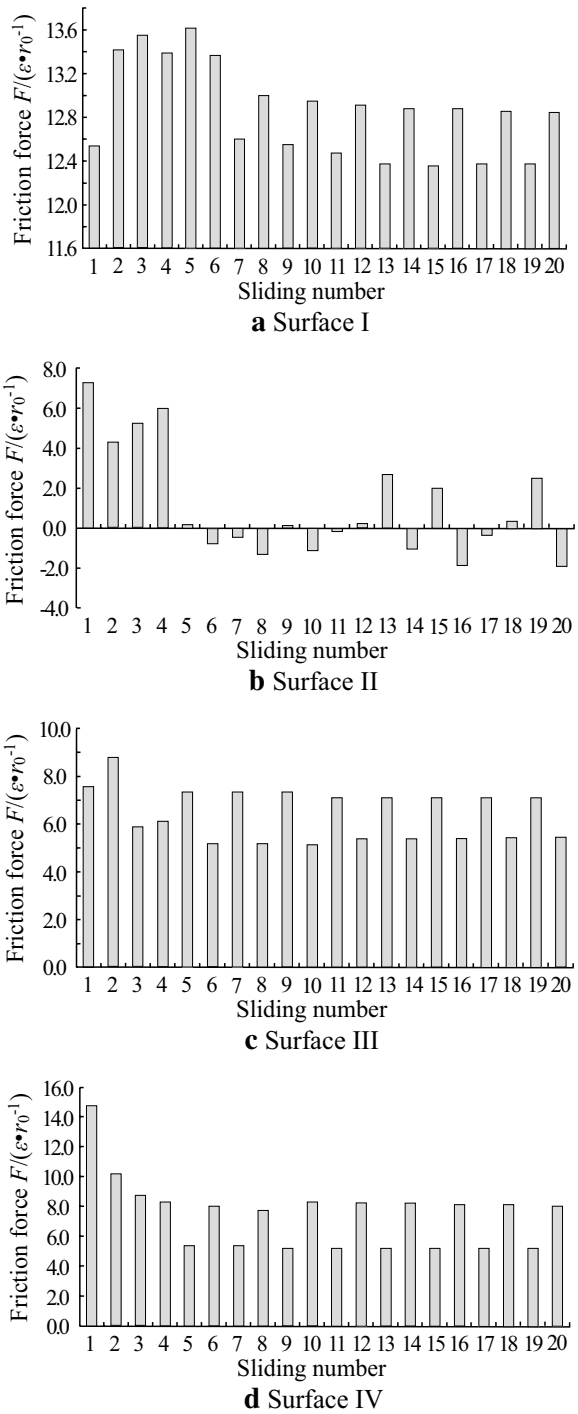

Figure 11 Nanoscale reciprocating sliding contacts of textured surfaces (7 textures, $R=60r_0$, $d=2.5r_0$)

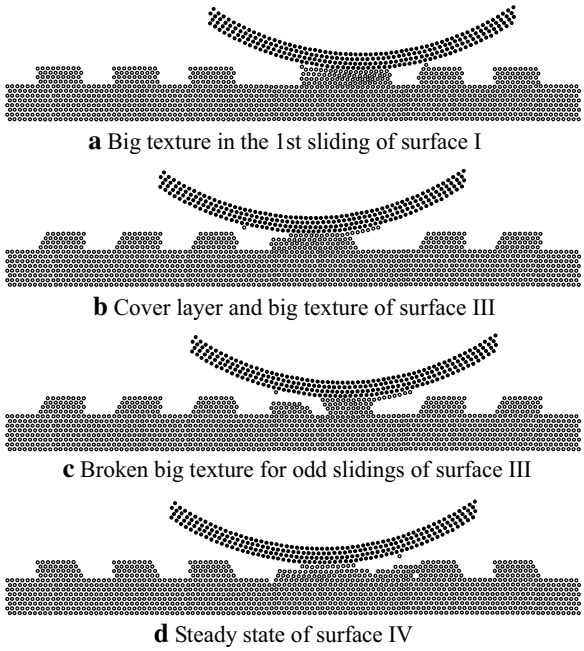

Figure 12 Structures during reciprocating sliding processes of textured surfaces (7 textures, $R=60r_0$, $d=2.5r_0$)

form a big texture again, and the average friction forces are lower compared with the cases of odd slidings.

The tip takes some atoms of the 4th texture to fill the spacing between the 4th and 5th textures in the 1st sliding for surface IV, and the spacing between the 5th and 6th textures is filled after the 3rd sliding. A big texture includes the 4th, 5th textures and the left part of the 6th texture is formed then, and the sliding comes to steady state from the 4th sliding. As shown in Figure 12(d), the big texture gets 2 layers, while the right part of the 6th texture includes 4 layers. Attractive forces act on the tip in the same direction as the sliding when the tip slides to right, so the average friction forces show low values. On the contrary, when the tip slides to left, the two directions are opposite, and the average friction forces are high.

When the tip radius is $R=120r_0$, average friction forces for different textures are shown in Figure 13. For surface I, the tip interacts with the 3rd, 4th, 5th and 6th textures. The 4th texture joins to the 5th texture when the 1st sliding is completed. As the beginning of the 2nd sliding, the tip takes the 6th texture and the big texture composed of the 4th and 5th textures to slide, and a big texture which contains these 4 textures is formed. During the following slidings, the big texture is changed all the time until steady slidings occur after the 13th sliding. From the 14th sliding, the tip breaks the big texture and takes part of it to slide for even slidings shown in Figure 14(a), while the tip takes the part to slide back for odd slidings shown in Figure 14(b). Forces to break the big texture make high average friction forces for even slidings, and low average friction forces are shown in odd slidings.

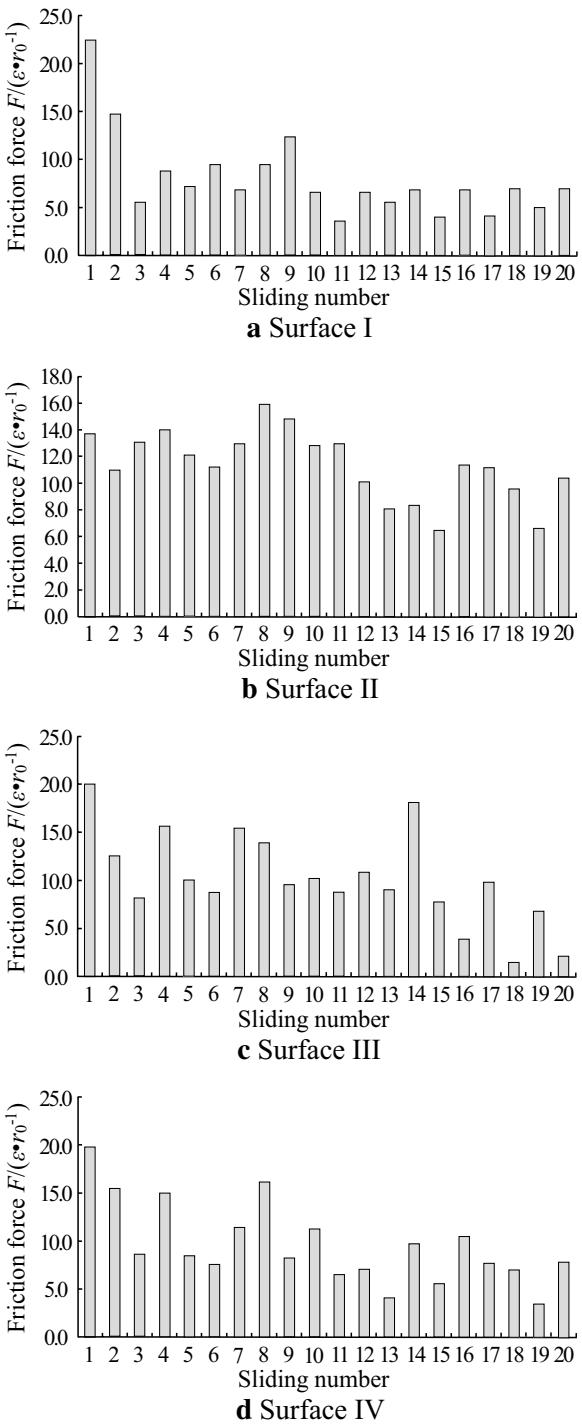

Figure 13 Nanoscale reciprocating sliding contacts of textured surfaces (7 textures, $R = 120r_0$, $d = 2.5r_0$)

For surface II, the tip takes part of the 3rd texture, the whole 4th and 5th textures to slide towards the 6th texture and scratches the 6th texture in the 1st sliding. Attractive forces between the tip and the textures are so high that most atoms adhere to the tip, and scratches between the tip and the textures occur occasionally. Besides, the textures and cover layer do not form stable structures, so the average friction forces fluctuate all the time.

The tip also interacts with the 3rd, 4th, 5th and 6th textures during the 1st sliding for surface III. When the 6th sliding is finished, a big texture is formed, and the tip takes some atoms to slide on the big texture to show high friction forces for the 7th and 8th slidings. From the 9th sliding, many atoms adhere to the tip, and the interactions between the tip and the big texture are slight, which induces low average friction forces. During the following slidings, more and more atoms accumulate on the right part of the tip, as shown in Figure 14(c), and the adhered atoms scratch the big texture to result in high average friction forces during the 14th sliding. Besides, the scratches make the adhered atoms move to the right part of the tip further, and no stable structure is formed, so the average friction forces fluctuate all the time.

For surface II, the tip takes part of the 3rd texture, the whole 4th and 5th textures to slide towards the 6th texture and scratches the 6th texture in the 1st sliding. Attractive forces between the tip and the textures are so high that most atoms adhere to the tip, and scratches between the tip and the textures occur occasionally. Besides, the textures and cover layer do not form stable structures, so the average friction forces fluctuate all the time.

The tip also interacts with the 3rd, 4th, 5th and 6th textures during the 1st sliding for surface III. When the 6th sliding is finished, a big texture is formed, and the tip takes some atoms to slide on the big texture to show high friction forces for the 7th and 8th slidings. From the 9th sliding, many atoms adhere to the tip, and the interactions between the tip and the big texture are slight, which induces low average friction forces. During the following slidings, more and more atoms accumulate on the right part of the tip, as shown in Figure 14(c), and the adhered atoms scratch the big texture to result in high average friction forces during the 14th sliding. Besides, the scratches make the adhered atoms move to the right part of the tip further, and no stable structure is formed, so the average friction forces fluctuate all the time.

For surface IV, the 4th, 5th and 6th textures join together to form a big texture in the 1st sliding, and the 3rd texture is also carried by the tip to slide together. The big texture is broken and the left part connects to the 3rd texture in the 2nd sliding. The broken and connection processes of the 4 layers big texture are continued until the end of the 8th sliding, and the average friction forces fluctuate greatly. Furthermore, the big texture consists of 1 layer or 2 layers then, and the tip takes atoms to slide on

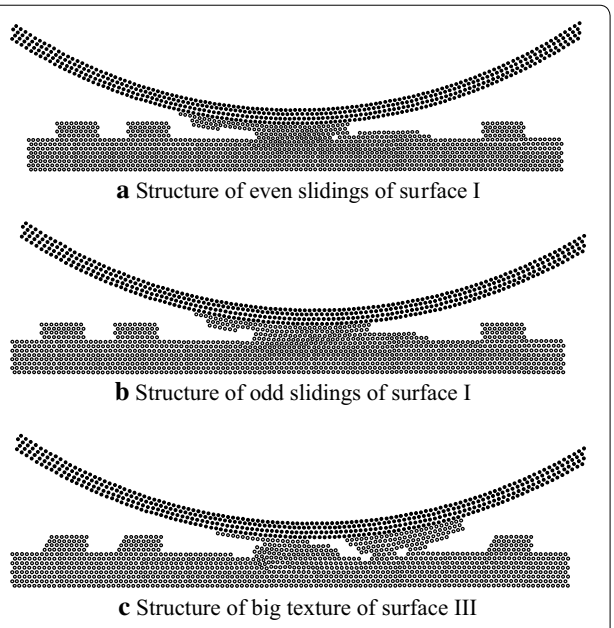

Figure 14 Structures during reciprocating sliding processes of textured surfaces (7 textures, $R=120r_0$, $d=2.5r_0$)

the big texture. The average friction forces become lower due to fewer atoms of the big texture.

From these 4 surfaces, only surface I comes to steady state, which is different from the cases of the tip radius $R=30r_0$ or $R=60r_0$. For the case of $R=120r_0$, adhesive effects are so marked that the tip takes too many atoms of the textures, and it is difficult to form a big texture on the substrate, so it is hard to make the sliding processes reach steady state. From this view, surface I gets the most atoms among the 4 surfaces, so a big texture can be formed and the average friction forces could be stable.

Comparing Figure 5, Figure 11 and Figure 13, one can find that the average friction forces of the 1st sliding increase as the increase of tip radii, which is similar to Ref. [20], while the subsequent average friction forces do not show regular trends. As the increase of tip radii, the surface whose texture contains more atoms will reach steady state, like surface I in Figure 11 and Figure 13. In Figure 6, Figure 12 and Figure 14, the worn atoms of $R=60r_0$ is the least, and the case of $R=120r_0$ is the most. So, the wear properties are affected by the combination of tip radius and textures.

3.4 Discussion

In this section, we tried to discuss the frictional properties from the view of the total average friction forces F_a during the whole sliding processes. Table 1 lists F_a for the cases of Section 3.1. On the whole, F_a increase with the indentation depth. Higher indentation depth induces higher ploughing component and also higher friction force.

Table 1 Total average friction forces for different indentation depth ($\varepsilon \cdot r_0^{-1}$)

Indentation depth	Surface I	Surface II	Surface III	Surface IV
$d=3.0r_0$	8.439	4.147	4.354	7.863
$d=2.5r_0$	5.215	1.277	5.136	2.981
$d=2.0r_0$	1.761	0.942	1.862	3.059

Table 2 Total average friction forces for different spacing ($\varepsilon \cdot r_0^{-1}$)

Spacing	Surface I	Surface II	Surface III	Surface IV
$7d_x$	5.215	1.277	5.136	2.981
$4d_x$	8.833	1.854	2.562	5.079

Table 3 Total average friction forces for different radii ($\varepsilon \cdot r_0^{-1}$)

Radii	Surface I	Surface II	Surface III	Surface IV
$R=30r_0$	5.215	1.277	5.136	2.981
$R=60r_0$	12.862	1.094	6.411	7.416
$R=120r_0$	7.984	11.321	10.117	9.569

For different texture spacings in Table 2, there is a trend that F_a increase as the spacings decrease, which is similar to the conclusions of Ref. [20]. When the spacings decrease, there are more atoms on the substrate, and the contact areas are higher to induce higher friction forces. Table 3 gives F_a for different tip radii. For most cases, F_a increase with the tip radii due to that bigger tip will induce higher contact areas and higher friction forces.

It should be noted that there are several cases which are not in accordance with the general trends. It is caused by the rearrangement of the atoms, and the variation of the structure during the sliding processes will influence the friction forces. In addition, when $d \geq 2.5r_0$, the ploughing components play the main role in friction forces, while the adhesion component plays the dominant role when $d<2.5r_0$, which may be another factor making the disaccords above. Furthermore, in nanoscale, contact area influences the friction forces significantly, which could be testified by the cases of different spacings and different tip radii.

Comparing these three tables, the lowest total average friction forces are mainly occurred on surface II. For the case of $R=60r_0$, surface II can reduce the total average friction force by 82.94%–91.49% compared with the other

three surfaces, so surface II should be a better choice to reducing friction forces.

4 Conclusions

(1) From the comparison of four surfaces with 7 textures at different indentation depths $d=2.0r_0$, $d=2.5r_0$ and $d=3.0r_0$, the lowest indentation depth can make all the four surfaces reach the steady state.
(2) Under the indentation depth $d=2.5r_0$, texture spacing does not show obvious influence on the average friction forces, and surfaces II, III and IV with 7 or 9 textures all reach steady state.
(3) Sliding processes are influenced by the combination of tip radius and texture shape. Except surface II, reciprocating sliding contacts between the tip with radius $R=60r_0$ and the surfaces with 7 textures can make the running-in stage shorter than other cases.
(4) In nanoscale, the total average friction forces of reciprocating sliding contact increase as the spacings decrease, and bigger tip radius will induce higher total average friction forces.
(5) The total average friction force can be reduced by 82.94%–91.49% for the combination of the tip with radius $R=60r_0$ and surface II.
(6) From the view of reaching steady state, surface III should be better for reducing the running-in stage. From the view of reducing total average friction forces, surface II will be a better choice. Besides, surface IV is the best to reduce wear.

Authors' Contributions

R-TT was in charge of the whole trial; R-TT wrote the manuscript; GL assisted with sampling and laboratory analyses. All authors read and approved the final manuscript.

Authors' Information

Rui-Ting Tong, born in 1981, is currently an associate professor at *Northwestern Polytechnical University, China*. He received his PhD degree from *Northwestern Polytechnical University, China*, in 2010. His research interests include nanoscale friction of texture surfaces, multiscale method, and contact mechanics, etc. Tel: +86-13892823204; E-mail: tongruiting@nwpu.edu.cn; nputongruiting@163.com.

Geng Liu, born in 1961, is currently a professor at *Northwestern Polytechnical University, China*. He received his PhD degree from *Xi'an Jiaotong Universtiy, China*, in 1992. His research interests include dynamics of mechanical system, tribology, contact mechanics, and planetary roller screw mechanism, etc. Tel: +86-29-88460411; E-mail: npuliug@nwpu.edu.cn.

Competing Interests

The authors declare that they have no competing interests.

Funding

Supported by National Natural Science Foundation of China (Grant Nos. 51675429, 51205313), Fundamental Research Funds for the Central Universities, China (Grant No. 3102014JCS05009) and the 111 Project, China (Grant No. B13044).

Publisher's Note

Received: 19 May 2016 Accepted: 2 August 2018
Published online: 14 August 2018

References

[1] P L Menezes, Kishore, S V Kailas. Studies on friction and formation of transfer layer when Al-4Mg alloy pins slid at various numbers of cycles on steel plates of different surface texture. *Wear*, 2009, 267(1–4): 525–534.
[2] P L Menezes, Kishore, S V Kailas, et al. The role of surface texture on friction and transfer layer formation during repeated sliding of Al-4Mg against steel. *Wear*, 2011, 271(9–10): 1785–1793.
[3] U Pettersson, S Jacobson. Influence of surface texture on boundary lubricated sliding contacts. *Tribology International*, 2003, 36(11): 857–864.
[4] A Kovalchenko, O Ajayi, A Erdemir, et al. Friction and wear behavior of laser textured surface under lubricated initial point contact. *Wear*, 2011, 271(9–10): 1719–1725.
[5] A Ramesh, W Akram, S P Mishra, et al. Friction characteristics of microtextured surfaces under mixed and hydrodynamic lubrication. *Tribology International*, 2013, 57(4): 170–176.
[6] M Scaraggi, F P Mezzapesa, G Carbone, et al. Minimize friction of lubricated laser-microtextured-surfaces by tuning microholes depth. *Tribology International*, 2014, 75(5): 123–127.
[7] N Morris, M Leighton, M De La Cruz, et al. Combined numerical and experimental investigation of the micro-hydrodynamics of chevron-based textured patterns influencing conjunctional friction of sliding contacts. *Proceedings of Institution of Mechanical Engineers Part J: Journal of Engineering Tribology*, 2015, 229(4): 316–335.
[8] H Z Fan, Y S Zhang, T C Hu, et al. Surface composition-lubrication design of Al_2O_3/Ni laminated composites—Part I: tribological synergy effect of micro-dimpled texture and diamond-like carbon films in a water environment. *Tribology International*, 2015, 84: 142–151.
[9] D Q He, S X Zheng, J B Pu, et al. Improving tribological properties of titanium alloys by combining laser surface texturing and diamond-like carbon film. *Tribology International*, 2015, 82(Part A): 20–27.
[10] M Bieda, C Schmädicke, T Roch, et al. Ultra-low friction on 100Cr6-steel surfaces after direct laser interference patterning. *Advanced Engineering Materials*, 2015, 17(1): 102–108.
[11] Q C Sun, T C Hu, H Z Fan, et al. Dry sliding wear behavior of TC11 alloy at 500℃: influence of laser surface texturing. *Tribology International*, 2015, 92: 136–145.
[12] W Z Wang, D Shen, S G Zhang, et al. Investigation of patterned textures in ball-on-disk lubricated point contacts. *ASME Journal of Tribology*, 2015, 137(1): 011502(1–12).
[13] K H Zum Gahr, M Mathieu, B Brylka. Friction control by surface engineering of ceramic sliding pairs in water. *Wear*, 2007, 263(11): 920–929.
[14] A Kovalchenko, O Ajayi, A Erdemir, et al. The effect of laser surface texturing on transitions in lubrication regimes during unidirectional sliding contact. *Tribology International*, 2005, 38(3): 219–225.
[15] K H Zum Gahr, R Wahl, K Wauthier. Experimental study of the effect of microtexturing on oil lubricated ceramic/steel friction pairs. *Wear*, 2009, 267(5–8): 1241–1251.
[16] W L Ma, J J Lu. Effect of surface texture on transfer layer formation and tribological behaviour of copper-graphite composite. *Wear*, 2011, 270(3–4): 218–229.
[17] H S Zhang, K Komvopoulos. Scale-dependent nanomechanical behavior and anisotropic friction of nanotextured silicon surfaces. *Journal of Materials Research*, 2009, 24(10): 3038–3043.
[18] H J Kim, D E Kim. Molecular dynamics simulation of atomic-scale frictional behavior of corrugated nano-structured surfaces. *Nanoscale*, 2012, 4(13): 3937–3944.
[19] J Li, Q H Fang, L C Zhang, et al. The effect of rough surface on nanoscale high speed grinding by a molecular dynamics simulation. *Computational Materials Science*, 2015, 98: 252–262.

[20] R T Tong, G Liu, T X Liu. Multiscale analysis on two dimensional nanoscale sliding contacts of textured surfaces. *ASME Journal of Tribology*, 2011, 133(4): 041401(1–13).
[21] N Mitchell, C Eljach, B Lodge, et al. Single and reciprocal friction testing of micropatterned surfaces for orthopedic device design. *Journal of the Mechanical Behavior of Biomedical Materials*, 2012, 7(1): 106–115.
[22] B Q Luan, S Hyun, J F Molinari, et al. Multiscale modeling of two-dimensional contacts. *Physical Review E*, 2006, 74(4): 046710(1–11).
[23] P M Agrawal, B M Rice, D L Thompson. Predicting trends in rate parameters for self-diffusion on FCC metal surfaces. *Surface Science*, 2002, 515(1): 21–35.
[24] J D Doll, H K Mcdowell. Theoretical studies of surface diffusion: self-diffusion in the FCC (111) system. *The Journal of Chemical Physics*, 1982, 77(1): 479–483.
[25] W C Swope, H C Andersen, P H Berens, et al. A computer simulation method for the calculation of equilibrium constants for the formation of physical clusters of molecules: application to small water clusters. *The Journal of Chemical Physics*, 1982, 76(1): 637–649.
[26] J Yang, K Komvopoulos. A molecular dynamics analysis of surface interference and tip shape and size effects on atomic-scale friction. *ASME Journal of Tribology*, 2005, 127(3): 513–521.
[27] D F Moore. *Principles and applications of tribology*. Oxford: Pergamon Press, 1975.